

Noise-based reward-modulated learning

Jesús García Fernández¹, Nasir Ahmad¹, and Marcel van Gerven¹

¹Department of Machine Learning and Neural Computing, Donders Institute for Brain, Cognition and Behaviour, Radboud University, Nijmegen, the Netherlands

Abstract

The pursuit of energy-efficient and adaptive artificial intelligence (AI) has positioned neuromorphic computing as a promising alternative to conventional computing. However, achieving learning on these platforms requires techniques that prioritize local information while enabling effective credit assignment. Here, we propose noise-based reward-modulated learning (NRL), a novel synaptic plasticity rule that mathematically unifies reinforcement learning and gradient-based optimization with biologically-inspired local updates. NRL addresses the computational bottleneck of exact gradients by approximating them through stochastic neural activity, transforming the inherent noise of biological and neuromorphic substrates into a functional resource. Drawing inspiration from biological learning, our method uses reward prediction errors as its optimization target to generate increasingly advantageous behavior, and eligibility traces to facilitate retrospective credit assignment. Experimental validation on reinforcement tasks, featuring immediate and delayed rewards, shows that NRL achieves performance comparable to baselines optimized using backpropagation, although with slower convergence, while showing significantly superior performance and scalability in multi-layer networks compared to reward-modulated Hebbian learning (RMHL), the most prominent similar approach. While tested on simple architectures, the results highlight the potential of noise-driven, brain-inspired learning for low-power adaptive systems, particularly in computing substrates with locality constraints. NRL offers a theoretically grounded paradigm well-suited for the event-driven characteristics of next-generation neuromorphic AI.

1 Introduction

Modern artificial intelligence (AI) models are growing exponentially, leading to proportional increases in their computational demands and energy consumption [44]. This trend, combined with the growing requirement for widespread AI deployment in local edge devices [52, 60], creates a massive demand for systems that are both fast and energy-efficient. Meeting this demand requires a fundamental shift in computing architecture to overcome the energy and latency bottlenecks of conventional Von Neumann systems [59]. Neuromorphic computing [50, 45, 29] offers a promising path forward by mimicking the low energy, event-driven, and parallel processing capabilities of the brain [50, 35]. Although neuromorphic hardware is highly efficient for inference, the ability to perform effective on-chip learning and adaptation remains the primary challenge, lacking suitable on-chip learning algorithms.

Backpropagation (BP) remains the workhorse algorithm for training artificial neural networks, computing precise global gradients for weight updates [46]. However, its operational requirements are fundamentally incompatible with the constraints of neuromorphic hardware [10]. BP requires precise global error propagation, which translates into high-bandwidth global data movement and large memory requirements to store activations, the main source of energy consumption in deep learning systems [36]. This contrasts sharply with the hardware needs for local synaptic updates that rely only on information available at the synaptic weight. In addition, BP's iterative forward and backward passes are incompatible with the asynchronous event-driven regime in which most neuromorphic devices operate [41], and its deterministic nature cannot tolerate inherent noise in neuromorphic circuits.

In response, local plasticity approaches and biologically-inspired learning rules have been proposed to bypass the constraints of BP [64, 63, 32, 47, 24, 67]. A particularly promising family of methods is noise-based learning, which leverages stochastic perturbations (either in weights [12, 69, 5, 9] or activations [18, 23, 65, 62, 15]) to approximate the true direction of the gradient. By injecting small

random perturbations, these methods avoid the need for perfectly matched feedback pathways and can leverage inherent noise [51, 35].

Given the prevalence of noise on neuromorphic and biological substrates [11, 53, 37], using noise as a mechanism to learn synaptic weights is an area of growing interest, with reward-modulated Hebbian learning (RMHL) [33, 38] as a promising candidate. RMHL, which is a form of three-factor Hebbian learning [20, 30], offers a potentially powerful mechanism for credit assignment without explicit backpropagation of errors. Despite theoretical advances, few noise-based methods have been adapted to real-world tasks. Some attempts which have been made include application to control problems [4], for spatiotemporal pattern generation [27], and for training non-differentiable spiking neural networks training [14], and these particularly struggle with delayed reward regimes. This gap has limited the integration of noise-based approaches for effective credit assignment in temporally extended setups.

To bridge these gaps, we propose noise-based reward-modulated learning (NRL), a biologically-inspired, gradient-free learning method, which is compatible with delayed feedback/rewards. We derive our learning rule from first principles, employing directional derivatives to compute a local gradient estimate at each synapse. These directional derivatives are implemented through stochastic neurons, aligning with the noisy nature of neuromorphic physical systems, and are estimated with two forward passes: a “noisy” pass with stochastic neurons and a “clean” pass without noise. In scenarios where a noiseless pass is infeasible, multiple noisy passes can be averaged to approximate the clean pass, maintaining performance as shown in our experiments. NRL draws from established neuroscientific concepts, by employing eligibility traces [22, 25], which tag synapses based on recent pre/post activity and noise perturbations, allowing retrospective credit assignment over behavioral timescales. It also incorporates reward prediction errors (RPEs), a dopamine-like signal [49, 48, 40] that modulates eligibility traces to reinforce actions that yield unexpected positive rewards, driving learning toward increasingly more advantageous behaviors. We deliberately utilize a rate-based neural model, instead of a spiking model, to focus the analysis on the core computational capabilities and limitations of the learning rule itself, making our findings immediately applicable to neuromorphic substrates.

We validate NRL on a suite of reinforcement-learning benchmarks that span immediate-reward and delayed-reward tasks, demonstrating significantly superior learning efficiency compared to RMHL (particularly when rewards were delayed by many steps) and competitive final performance compared to the gradient-based baseline. Moreover, unlike RMHL, which breaks down in deeper architectures, NRL scales to multilayer networks, though converging more slowly due to its intrinsic stochasticity.

Our findings argue that NRL represents a promising and scalable step toward developing low-energy and fast adaptive AI systems. By transforming the stochasticity of neuromorphic hardware from a challenge into a computational resource, NRL provides a crucial new algorithmic path for enabling complex, continuous learning at the edge, as well as novel, alternative, robust learning schemes for machine learning.

2 Methods

2.1 Neural system-environment interaction and reward signaling

We model a neural system within a dynamic environment, grounded in the reinforcement learning framework [56]. In this framework, the state of the environment at time t is denoted by s_t . The neural system perceives s_t and responds by initiating actions a_t , which influence the environment. Each action or sequence of actions results in feedback in the form of positive or negative rewards r_t . This iterative process of perception, action, and outcome forms a feedback loop that enables the system to learn and adapt to the changing environment, ultimately seeking to maximize the rewards it receives.

The decision-making of the system is guided by a policy π , which represents the probability of choosing an action, a_t , in a given state s_t at time t , i.e., $\pi(a_t | s_t)$. This policy captures the system’s learned strategy for choosing actions that are likely to yield favorable outcomes. To determine an action, the system computes a probability distribution across the set of possible actions, modeled as a categorical distribution $P(a_t | s_t) \equiv \pi(a_t | s_t)$ with $\sum_{a \in A} \pi(a | s_t) = 1$, where A denotes the set of all possible actions.

The rewards r_t , obtained from the environment, serve as crucial learning signals. Internally, the system maintains a prediction of the expected reward, denoted by \bar{r}_t . Although this prediction can be calculated through various mechanisms, we model it here for simplicity as a running average of recent

rewards as

$$\bar{r}_{t+1} = \bar{r}_t + \lambda(r_{t+1} - \bar{r}_t) \quad (1)$$

where λ is a smoothing factor that governs the influence of past rewards on the current prediction. The mismatch between the actual reward and the predicted reward, known as the reward prediction error, is then computed as

$$\delta_t = r_t - \bar{r}_t. \quad (2)$$

This RPE signal, which draws a strong parallel to the phasic activity of dopamine neurons in the brain [49, 48, 40, 16], functions as a low-bandwidth global feedback signal that is inherently compatible with the communication constraints of neuromorphic hardware. Although our running average is a simplified representation of how reward expectations are formed, it effectively captures the fundamental dynamics of the RPE and its role as an adaptive learning signal. We will explore potential refinements of this reward prediction mechanism in the Discussion section.

2.2 Derivation of the learning rule

This section presents a complete derivation of the NRL update rule. We begin by establishing a gradient-based learning rule rooted in an optimization target that aims to maximize unexpected rewards from the environment by increasing the reward prediction error. Using RPE, rather than direct reward, enables our system to adapt dynamically to changing environments by tracking how rewards deviate from expectations, improving long-term performance by continuously seeking rewards that exceed expectations, and maintaining robustness against variations in reward structures [56, 42].

Building on this foundation, we transition to a directional derivative framework, where intrinsic noise within the network is leveraged to approximate gradients. This critical step eliminates the need for backpropagation and feedback phases, enabling learning through forward passes alone. Finally, we extend our noise-based approach to handle scenarios with delayed rewards, a hallmark of real-world problems. This extension enables NRL to adapt to environments where feedback is obtained only after a series of actions.

2.2.1 Gradient-based learning rule

The system is modeled as a multi-layered network of interconnected units, analogous to populations of neurons, which processes input representing sensory observations and produces a probability distribution over possible actions. For simplicity, we refer to these populations as ‘layers,’ where each layer performs a transformation of its input in two stages: first, a linear transformation, followed by a non-linear transformation. This can be expressed mathematically as

$$x_t^l = f(h_t^l) = f(W_t^l x_t^{l-1}) \quad (3)$$

where x_t^l represents the output activity of layer l , h_t^l represents the layer pre-activation (the combined input to such layer), W_t^l represents the matrix of synaptic weights connecting layer $l - 1$ to layer l , at time t , and $f(\cdot)$ is a non-linear activation function, which introduces crucial non-linearities into the network’s computations

In this setup, the goal is to adjust the synaptic weights, $\{W^1, \dots, W^L\}$, across the L layers of the network to maximize the rewards obtained by the system. Our derivation begins by introducing a general parameter θ , which will later be mapped to the specific neural network parameters W . The primary learning objective is to maximize the RPE, δ_t , at any particular moment in time, t , effectively driving the system to seek out actions that lead to higher-than-predicted rewards. The reward prediction is modeled as a running average of recent rewards and, as such, the learning rule seeks to outperform previously received rewards. Note that for a fixed reward prediction, this is equivalent to maximizing the reward itself. We express this objective in terms of a parameterized policy at time t as

$$J(\theta_t) = \mathbb{E}_{\pi_{\theta_t}} [\delta_t]. \quad (4)$$

To optimize $J(\theta_t)$, we can incrementally update the weights using the gradients with respect to θ_t as

$$\theta_{t+1} \leftarrow \theta_t + \eta \nabla J(\theta_t) \quad (5)$$

where η is the learning rate, controlling the size of each update step.

Applying the policy gradient theorem [57], which utilizes the likelihood-ratio method, we express the gradient of the objective as

$$\nabla J(\theta_t) = \mathbb{E}_{\pi_{\theta_t}} [\nabla \log \pi_{\theta_t}(a_t | s_t) \delta_t] .$$

For empirical estimation, in the case of a single sample, we approximate the gradient as $\nabla J(\theta_t) \approx \nabla \log \pi_{\theta_t}(a_t | s_t) \delta_t$. Using this approximation, we define the parameter updates as

$$\theta_{t+1} \leftarrow \theta_t + \eta \nabla \log \pi_{\theta_t}(a_t | s_t) \delta_t . \quad (6)$$

Equation (6) resembles the REINFORCE update rule [65] but differs by using the reward prediction error, δ_t , as the learning signal instead of cumulative rewards over full trajectories. This RPE-based approach leverages immediate feedback from rewards as they are obtained rather than requiring a full trial completion to estimate the policy gradient. It shares conceptual similarities with actor-critic methods in reinforcement learning [1], where the policy is adjusted using a temporal difference error. However, we approximate future rewards with a running average of past rewards instead of a critic network, a less powerful but simpler implementation which maintains adaptive feedback.

2.2.2 Noise-based learning rule

The learning rule derived in the previous section still relies on gradient descent. To avoid using back-propagation to compute the gradients, we propose a noise-based alternative that extends Equation (6). This approach leverages gradient approximation via directional derivatives, enabling a theoretically rigorous derivation of noise-driven learning.

A directional derivative quantifies the rate of change of a function in a specified direction. In our neural system, we implement this concept by introducing random noise into parameters. By comparing the network’s parameters with and without this noise, we obtain an estimate of the gradient direction. To formalize this, we define $g(\theta_t) = \log \pi_{\theta_t}(a_t | s_t)$ and express the gradient term in terms of directional derivatives using the theorems in Appendix A as

$$\nabla g(\theta_t) = \nabla \log \pi_{\theta_t}(a_t | s_t) = n \mathbb{E} [\bar{\epsilon}_t \nabla_{\bar{\epsilon}_t} g(\theta_t)] \quad (7)$$

where $\bar{\epsilon}_t = \epsilon_t / \|\epsilon_t\|$ is a normalized direction vector derived from noise $\epsilon_t \sim \mathcal{N}(0, \sigma^2 I_n)$ with n the number of parameters.

We may expand the above to approximate the gradient via a finite-difference and by sampling under an empirical distribution

$$\nabla g(\theta_t) \approx n \sum_{i=1}^K \left[\frac{\epsilon_t^{(i)}}{\|\epsilon_t^{(i)}\|^2} \left(g(\tilde{\theta}_t^{(i)}) - g(\theta_t) \right) \right] \quad (8)$$

where K denotes the number of samples and $\tilde{\theta}_t^{(i)} = \theta_t + \epsilon_t^{(i)}$ the noise-perturbed parameters (see Appendix A). In practice, we consider $K = 1$, analogous to single-sample updates in stochastic gradient descent. Here, $g(\tilde{\theta}_t^{(i)}) = \log \pi_{\tilde{\theta}_t^{(i)}}(a_t | s_t)$ and $g(\theta_t) = \log \pi_{\theta_t}(a_t | s_t)$ are the log of the noise-perturbed and noise-free output, respectively. Thus, we define $\rho_t = \log \pi_{\tilde{\theta}_t}(a_t | s_t) - \log \pi_{\theta_t}(a_t | s_t)$, which captures the impact of the noise on the policy. Putting this together for the $K = 1$ case, we obtain our noise-based learning rule

$$\theta_{t+1} \leftarrow \theta_t + \eta \delta_t \hat{\epsilon}_t \rho_t$$

with $\hat{\epsilon}_t = \epsilon_t / \|\epsilon_t\|^2$. For convenience, we absorbed the term n into the learning rate η .

2.2.3 Learning with node level noise in neural network

The noise-based learning rule derived so far is formulated for a general parameter θ_t . Now, we apply this framework to the specific context of a neural network, where θ_t corresponds to the synaptic weights W_t^l of layer l at time t .

Instead of directly perturbing the weights of the network W_t^l , we propose introducing noise directly into the neurons (nodes) of each layer. This strategy is advantageous because it leads to reduced variance in gradient estimation, as perturbations occur in a lower-dimensional space (the neural activations) compared to the full weight space. In addition, it naturally reduces the computational cost and communication overhead associated with high-dimensional perturbations. This approach shares similarities with node perturbation (NP) [18, 23, 65, 62, 15], which has shown benefits in reducing gradient variance and offering more localized updates.

Given a layer transformation as in Equation (3), adding noise at the neuron level is represented as

$$\tilde{x}_t^l = f\left(\tilde{h}_t^l + \xi_t^l\right) = f\left(W_t^l(\tilde{x}_t^{l-1})^\top + \xi_t^l\right) \quad (9)$$

where $\xi_t^l \sim \mathcal{N}(0, \sigma^2 I_{m^l})$ is the injected noise at time t , σ^2 is some arbitrarily small noise scale, and m^l is the number of neurons in layer l . We use the notation \tilde{x}_t^l and \tilde{h}_t^l to denote perturbed inputs and pre-activations, respectively, which may also result from perturbations of previous network layers on which layer l depends.

To formulate the learning rule for specific layer parameters $W_t^l \in \{W_t^1, \dots, W_t^L\}$, we re-express the gradient in terms of the pre-activations instead of the parameters themselves. Here, the general parameter vector $\theta_t = \{W_t^1, \dots, W_t^L\}$ corresponds to the full set of all weight matrices for all layers at time t . To do so, we first rewrite the gradient term as

$$\nabla g(W_t^l) = \nabla \log \pi_{\theta_t}(a_t | s_t) \quad (10)$$

and apply the chain rule to break down the gradient with respect to W_t^l as

$$\nabla g(W_t^l) = \nabla g(h_t^l) \frac{\partial h_t^l}{\partial W_t^l} = \nabla g(h_t^l) (x_t^{l-1})^\top. \quad (11)$$

Notably, we may once again carry out the conversion from this gradient estimation step to a set of directional derivatives such that

$$\nabla g(h_t^l) (x_t^{l-1})^\top \approx n \sum_{i=1}^K \left[\frac{\xi_{t,i}^l}{\|\xi_{t,i}^l\|^2} \left(g(\tilde{h}_{t,i}^l) - g(h_t^l) \right) \right] (x_t^{l-1})^\top \quad (12)$$

where i indexes over a set of repeated samples of the noise term, ξ .

Again, as above, by reducing this to the single sample ($n = 1$) case, we can define a layer-specific weight update rule

$$W_{t+1}^l \leftarrow W_t^l + \eta \delta_t \bar{\xi}_t^l \rho_t (\tilde{x}_t^{l-1})^\top \quad (13)$$

with $\rho_t = \log \pi_{\tilde{W}_t}(a_t | s_t) - \log \pi_{W_t}(a_t | s_t)$ and $\bar{\xi}_t^l = \xi_t^l / \|\xi_t^l\|^2$. Here, $\pi_{\tilde{W}_t}(a_t | s_t)$ represents the network's output when noise is injected into the neurons, while $\pi_{W_t}(a_t | s_t)$ corresponds to the output of the noiseless network. This form of the noise-based learning rule is directly applicable in settings with continuous reward signals.

2.2.4 Learning from sparse rewards

Our derivations so far assume that synaptic updates happen at every time step, implying a continuous stream of rewards and learning signals. In reality, however, rewards are often sparse, arriving only after a sequence of actions or upon reaching specific milestones. To handle this, we'll modify our learning rule to account for rewards received at arbitrary times.

Let us denote these discrete reward times as $\tau_m \in \{\tau_0, \tau_1, \dots, \tau_M\}$. At these moments, we compute the RPE as

$$\delta_{\tau_m} = r_{\tau_m} - \bar{r}_{\tau_m}. \quad (14)$$

Here, r_{τ_m} is the reward received at time τ_m , and \bar{r}_{τ_m} is the reward prediction, which is updated as the running average of recent rewards:

$$\bar{r}_{\tau_m} = \bar{r}_{\tau_{m-1}} + \lambda (r_{\tau_m} - \bar{r}_{\tau_{m-1}}). \quad (15)$$

While synaptic updates only occur at these specific reward times τ_m , the learning rule continuously accumulates information between rewards. This information is integrated over time, allowing us to update weights based on what’s happened since the last reward. This leads to our modified learning rule

$$W_{\tau_m}^l \leftarrow W_{\tau_{m-1}}^l + \eta \delta_{\tau_m} e_{\tau_m} \quad (16)$$

where

$$e_{\tau_m} = \sum_{t=\tau_{m-1}}^{\tau_m} \bar{\xi}_t^l \rho_t (\tilde{x}_t^{l-1})^\top \quad (17)$$

is an eligibility trace that acts as a mechanism to connect past actions with future rewards [22]. Eligibility traces capture neural activity and other local variables over time, signaling potential synaptic changes. Upon receiving a reward, these traces are modulated by the reinforcement signal, resulting in synaptic updates. Some models view eligibility traces as decaying cumulative activity [25, 56]), while others treat them as a full activity history [38], which aligns with our formulation. The eligibility trace efficiently tracks neural information between rewards, facilitating the assignment of credit to past actions.

Thus, our final learning rule consists of two primary components: (i) an eligibility trace, defined in Equation (17), which accumulates local information over time at each time step, and (ii) a synaptic update, defined in Equation (16), triggered upon reward receipt, which modulates the eligibility trace to adjust the synaptic weights. This learning rule constitutes the core of our proposed noise-based reward-modulated Learning (NRL) and is used for all experiments presented in this paper.

2.3 Neural network architecture

The learning and decision-making capabilities of the system are modelled using a feedforward network with L layers, representing interconnected populations of neurons. The transformation performed by each hidden layer at time t can be expressed as

$$\tilde{x}_t^l = f (W_t^l (\tilde{x}_t^{l-1})^\top + \xi_t^l) \quad (18)$$

and the readout in the output layer is given by

$$\tilde{y}_t = s (W_t^l (\tilde{x}_t^{l-1})^\top + \xi_t^l) \quad (19)$$

where x_t^l represents the activity of units in layer l , W_t^l is the matrix of synaptic weights connecting layer $l - 1$ to layer l , and $\xi_t^l \sim \mathcal{N}(0, \sigma^2 I_{m^l})$ represents random noise introduced into layer l , with m^l being the number of units in such layer. This noisy propagation of activity is termed a “noisy pass.” The function $f(\cdot)$ is a non-linear activation function, which we implement as the LeakyReLU function such that $f(x) = x$ if $x \geq 0$ and $f(x) = \alpha x$ with $0 < \alpha \ll 1$. The function $s(\cdot)$ represents a softmax transformation $s_i(x) = e^{x_i} / \sum_{j=1}^{m^l} e^{x_j}$, which transforms the network’s output into a probability distribution over possible actions. We also define a “clean pass,” representing the network’s activity in the absence of noise, by $x_t^l = f (W_t^l (x_t^{l-1})^\top)$ and $y_t = s (W_t^l (x_t^{l-1})^\top)$.

2.4 Experimental validation

We validate our approach across a range of simulated environments, comparing it against established baseline learning methods. Each environment presents a problem with discrete episodes, where the system’s learning is guided solely by positive or negative rewards. We investigate both scenarios with immediate reward and those involving delayed reward. In the delayed reward scenarios, a single reward is provided after a sequence of actions, challenging our system to assign credit retrospectively to the actions that contributed to the outcome. For the instantaneous reward setting, we use the Reaching

problem [21], while the delayed reward setting uses the Cartpole [1] and Acrobot [55] problems. We use implementations given by the libraries OpenAI Gym [3] and NeuroGym [39] for the different environments.

We compare NRL to two baselines: an exact-gradient version of NRL, which serves as an "optimal performance" benchmark, and an RMHL approach.

The first baseline, which we refer to as the exact-gradient method (BP baseline), is similar to an actor-only variant of actor-critic methods, relying on a running average of past rewards as the prediction error. For this baseline, we compute the exact policy gradients for the entire episode trajectory using backpropagation through time (BPTT) [61]. Given sparse rewards, the weights at each layer are updated at the end of each episode according to

$$W_{\tau_m}^l \leftarrow W_{\tau_{m-1}}^l + \eta \left(\nabla_{W_{\tau_{m-1}}^l} \log \pi_{\theta_{\tau_{m-1}}}(a_t | s_t) \right) \delta_{\tau_m}. \quad (20)$$

The second baseline, motivated by the noise-based nature of NRL, is the RMHL rule from [33] with an explicit-noise approximation – the original version where noise is inferred from neural activities proved too unstable for the problems considered here. For delayed rewards, we adapt it similarly to [38], updating eligibility traces as

$$e_{\tau_m} = \sum_{t=\tau_{m-1}}^{\tau_m} \xi_t^l (\tilde{x}_t^{l-1})^\top. \quad (21)$$

Similar to NRL’s noise-based learning rule defined in Equation (16), the synaptic weights for RMHL are then updated by modulating this eligibility trace with the reward prediction error.

In Table 1, we present the complete three learning rules (NRL, BPTT, and RMHL) in a single table for visualization and quick comparison. All updates are written in a per-layer form using W^l and assume a delayed reward received at time τ_m .

Table 1: Learning rules. The terms in the BPTT update are rearranged for easier comparison.

| Rule | Update |
|------|--|
| NRL | $W_{\tau_m}^l \leftarrow W_{\tau_{m-1}}^l + \eta \delta_{\tau_m} \sum_{t=\tau_{m-1}}^{\tau_m} \bar{\xi}_t^l \rho_t (\tilde{x}_t^{l-1})^\top$ |
| BPTT | $W_{\tau_m}^l \leftarrow W_{\tau_{m-1}}^l + \eta \delta_{\tau_m} \nabla_{W_{\tau_{m-1}}^l} \log \pi_{\theta_{\tau_{m-1}}}(a_t s_t)$ |
| RMHL | $W_{\tau_m}^l \leftarrow W_{\tau_{m-1}}^l + \eta \delta_{\tau_m} \sum_{t=\tau_{m-1}}^{\tau_m} \xi_t^l (\tilde{x}_t^{l-1})^\top$ |

In environments with high reward variability, like Cartpole and Acrobot, we stabilize synaptic updates by scaling the RPE by dividing by r_{τ_m} . Hyperparameter values and training details are provided in Appendix B. All experiments are implemented in Python using PyTorch [43]. Our models and scripts are available for reproducibility at <https://github.com/jesusgf96/noise-based-reward-modulated-learning>.

3 Results

3.1 Performance on control tasks with instantaneous and delayed rewards

To ensure comparability with RMHL methods, which typically utilize single-hidden-layer networks, we first conduct experiments with a one-hidden-layer neural network for BP, NRL, and RMHL. Training details are provided in Appendix B. In Section titled "Scalability to deeper architectures", we extend the comparison to deeper networks with multiple hidden layers.

First, the Reaching problem [21], visualized in Fig. 1C, is an immediate reward problem that requires the system to reach and maintain a position at a target on a 1D ring by moving left, right, or remaining stationary. At each step, the system receives information about both the target’s position

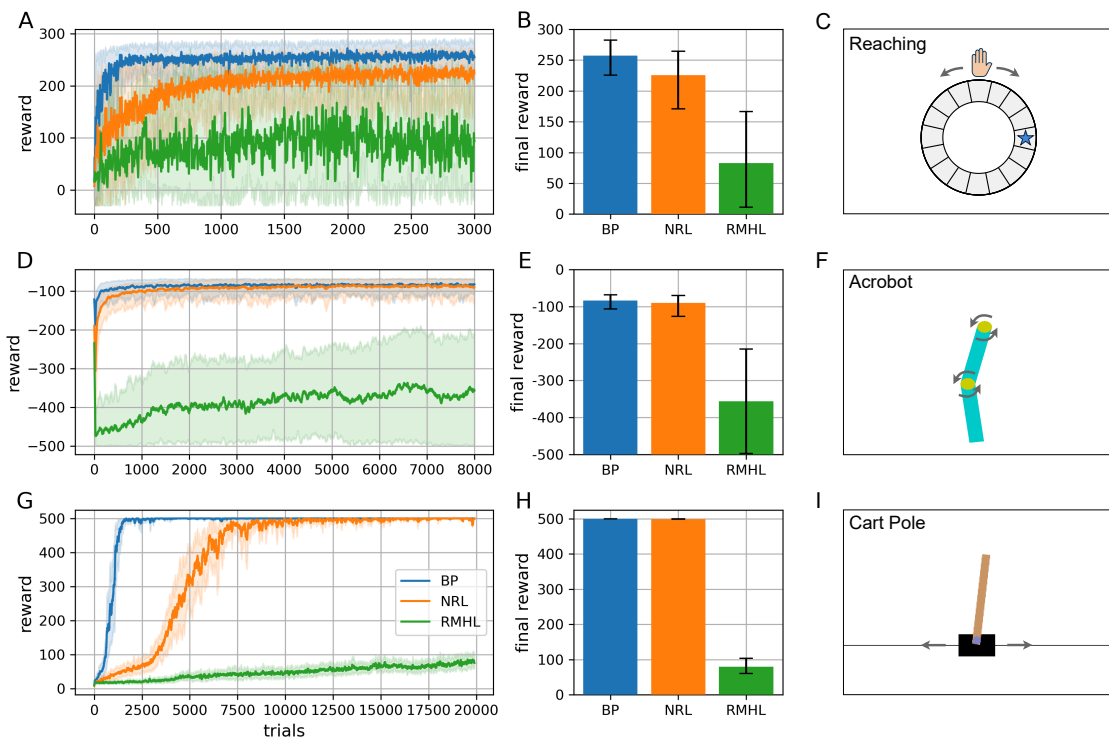


Figure 1: **Performance on benchmarks.** A, B, C: Reaching problem. D, E, F: Acrobot problem. G, H, I: Cartpole problem. Left panels: Performance across trials averaged over 5 runs. Centre panels: Final performance (mean of the last 50 trials), averaged over 5 runs. Right panels: Problem visualization.

and its own, and a reward is provided based on proximity to the target over fixed-duration trials. Average performance across-trial and final performance (mean of the last 50 trials) are shown in Fig. 1A and Fig. 1B, respectively.

Second, the Acrobot problem [55], visualized in Fig. 1F, involves delayed reward and requires controlling a two-link robotic arm to reach a target height. At each time step, the system receives information about the angles and angular velocities of the two links and chooses one action: clockwise torque, counterclockwise torque, or no torque. Rewards are given based on the speed of completion, with a maximum time allowed. Average performance across trials and final performance (mean of the last 50 trials) are shown in Fig. 1D and Fig. 1E, respectively.

The third and most challenging problem, the Cartpole problem [1], visualized in Fig. 1I, is a delayed reward problem where the system must balance a pole on a cart by moving left or right. At each time step, the system receives information about the cart’s position and velocity, along with the pole’s angle and angular velocity, and responds accordingly. Performance is measured by the time the pole remains balanced, with a maximum time allowed. Average performance across trials and final performance (mean of the last 50 trials) are shown in Fig. 1G and Fig. 1H, respectively. For all three tasks, NRL achieves a final performance comparable to the gradient-based baseline, BP, demonstrating a vast difference compared to RMHL.

3.2 Scalability to deeper architectures

Here, we demonstrate that NRL can effectively assign credit in neural networks with multiple hidden layers; a challenging scenario where most biologically plausible algorithms struggle. We use both the Acrobot and the Cartpole tasks for this purpose, as they present a delayed reward problem, making them a more realistic test for credit assignment in reinforcement learning. In this comparison, we include the same baselines, BP and RMHL. Figure 2 displays the results for the Acrobot task and Fig. 3 displays the results for the Cartpole tasks for neural networks consisting of two and three hidden

layers. The left panels of these two figures show performance across trials, averaged over 5 runs. In contrast, the right panels display the final performance (mean of the last 50 trials), also averaged over 5 runs.

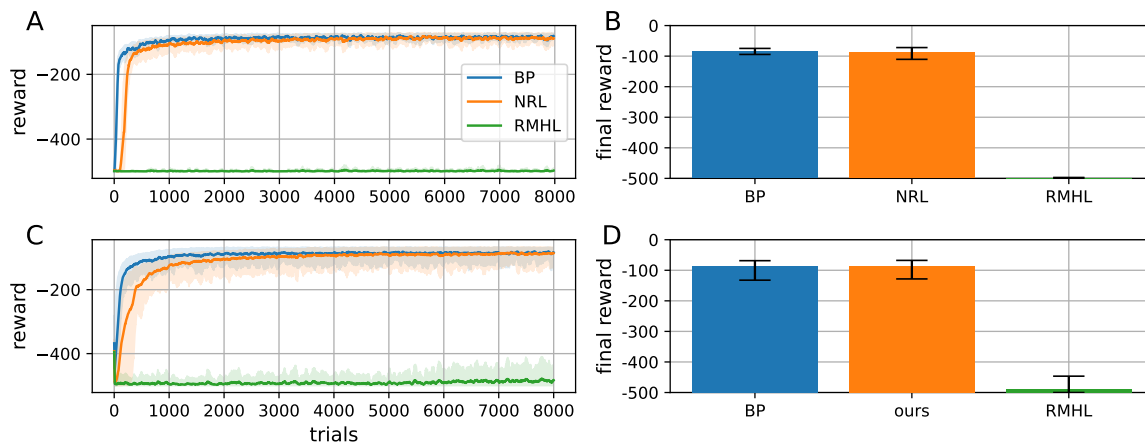


Figure 2: **Performance on deeper networks for the Acrobot.** A, B: 2-hidden layer networks. C, D: 3-hidden layer networks. Left panels: Performance across trials averaged over 5 runs. Right panels: Final performance (mean of the last 50 trials), averaged over 5 runs.

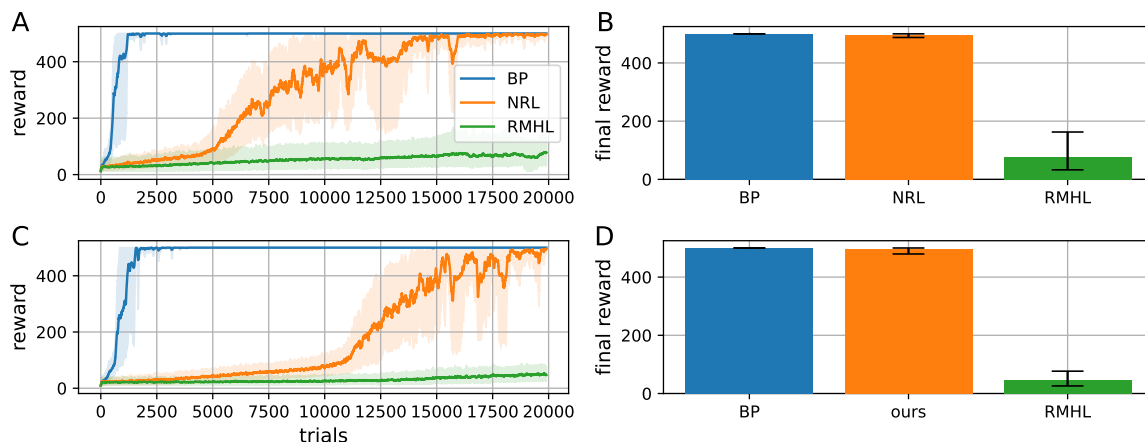


Figure 3: **Performance on deeper networks for the Cartpole.** A, B: 2-hidden layer networks. C, D: 3-hidden layer networks. Left panels: Performance across trials averaged over 5 runs. Right panels: Final performance (mean of the last 50 trials), averaged over 5 runs.

Our results indicate that NRL successfully learns to solve the tasks, achieving performance comparable to BP. In contrast, RMHL struggles with credit assignment in deeper networks. However, NRL requires more trials to converge as the network depth increases, which is an expected outcome due to the stochastic nature of the updates [23]. A similar trend is observed with BP, though to a lesser extent, as its gradient-based updates inherently provide more directed adjustments.

3.3 Learning using only noisy passes

In NRL, ρ_t is calculated as the difference in the network’s output between the clean and noisy passes. However, generating a perfectly noiseless pass may be hardware-infeasible or energy-prohibitive in neuromorphic circuits. Instead, we show that the clean network’s output can be approximated by averaging the outputs from multiple noisy passes, as the injected noise averages to zero $\lim_{N \rightarrow \infty} \frac{1}{N} \sum_{i=1}^N \xi_{t,i}^l = 0$.

This assumes that the network dynamics are faster than the environment dynamics, allowing the network to perform multiple forward passes before the environment changes.

To evaluate the accuracy of this approximation, we employ a single hidden-layer network and the Acrobot problem. The difference between the clean pass output and the averaged noisy passes output was calculated for each timestep and averaged over 500 timesteps, as shown in Fig. 4A. Furthermore, Fig. 4B illustrates the performance on the Acrobot problem using only noisy forward passes, starting with a minimum of 2 noisy passes. We also extended this evaluation to 10 noisy passes to explore the impact of increasing the number of passes, showing slightly faster initial convergence.

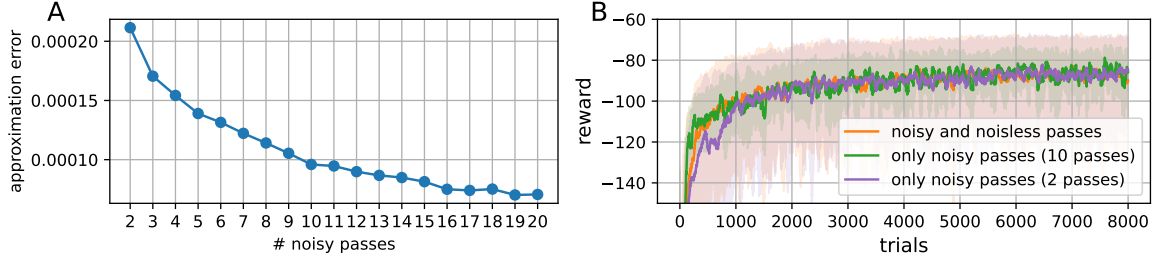


Figure 4: **Learning using only noisy passes for the Acrobot.** A: Clean pass approximation error. Each data point is computed with an absolute error, averaged over 500 timesteps using the Acrobot problem. B: Acrobot problem. Performance across trials, averaged over 5 runs, with mean, minimum, and maximum values displayed.

4 Discussion

In this work, we propose NRL, noise-based reward-modulated learning, a novel synaptic plasticity rule that bridges the principles of reinforcement learning and optimization with biologically inspired Hebbian updates. By leveraging stochastic neural activity, our method produces local synaptic updates modulated by a global reinforcement signal. It offers an efficient approach for neural adaptation, particularly suited to neuromorphic systems.

We employ a top-down methodology, deriving our learning rule from the mathematical principles of gradient-based optimization. We approximate the gradients through directional derivatives and incorporate bottom-up constraints inspired by biological systems. Specifically, the gradient-approximation process is implemented through stochastic neural activity, directly aligning with the inherent noise in neuromorphic substrates [50, 45, 29] and the brain [11, 53, 37]. Reinforcement learning mechanisms are realized through reward prediction errors (emulating dopaminergic reward signals [49, 48]), eligibility traces, and local synaptic plasticity. These elements also enable learning under uncertainty [17]. This approach results in a learning rule that is both theoretically grounded and potentially realizable in event-driven neuromorphic hardware.

Our results demonstrate the learning effectiveness of NRL, solving both immediate and delayed feedback/reward problems in simulated environments, achieving performance comparable to baselines optimized employing backpropagation. In addition, it shows a significant improvement over RMHL [33, 38], a modern approach that also uses noise as the core of its synaptic plasticity. Our scalability results further demonstrate that NRL effectively assigns credit even in multilayer networks, a challenge for many biologically plausible or local algorithms, indicating its potential for scaling. This is a critical difference from RMHL, which struggles to assign credit in multilayer networks, as evidenced by its minimal performance improvements across trials. Nevertheless, as the depth of the network increases, NRL shows slower convergence due to its noise-driven updates.

NRL shares similarities with node perturbation methods [18, 23, 65, 62, 15], which inject noise into neurons to adjust weights based on state and performance fluctuations. However, unlike node perturbation, which requires constant feedback or reward for learning, NRL is well-suited for delayed reward setups. By leveraging eligibility traces [22, 25], it can effectively assign credit to past neural states even when actions and outcomes are separated in time.

Gradient approximation, a cornerstone of our learning rule’s derivation, is also crucial in mathematical optimization and machine learning, enabling learning when exact gradients are computationally expensive or unavailable. Techniques such as forward gradient methods [2] and zeroth-order optimization [34, 6] have emerged, utilizing stochastic perturbations and function value comparisons to estimate gradients. Recent advances, such as employing local auxiliary networks for informed gradient guesses [19], have significantly improved the alignment of these approximations with exact gradients, reducing the performance gap with backpropagation. These variance-reduction strategies could similarly enhance our approach by improving the quality of the updates and scalability to more complex architectures. Furthermore, compared to traditional gradient-based methods like backpropagation, gradient approximation methods offer a key advantage in computationally constrained scenarios, or when using non-differentiable networks, such as spiking neural networks [66, 58].

Additionally, the local-update structure of NRL provides direct compatibility with neuromorphic substrates [50], where only locally available information in the synapse is prioritized and global communication is severely penalized. This eliminates the need for the high-bandwidth global data movement and large memory buffers required by backpropagation, the primary source of energy consumption in deep learning models, addressing the fundamental energy and latency bottlenecks of conventional Von Neumann systems. Furthermore, NRL’s reliance on noise for gradient approximation offers a paradigm shift: it transforms the device stochasticity common in neuromorphic circuits from an engineering challenge into a computational resource. The inherent noise in NRL is also advantageous for reinforcement learning setups, as it naturally facilitates the exploration-exploitation balance [26, 31]. Injected noise perturbs neural states, promoting exploratory deviations from expected values and thus introducing variations in the agent’s policy, which benefits adaptation on neuromorphic edge devices.

Despite its promise, our work has limitations that suggest future research directions. The current requirement for multiple forward passes (noisy and clean) per synaptic update, while theoretically simple, introduces a time-latency overhead. Future work should explore more efficient ways to estimate noise impacts, potentially eliminating the need for multiple passes. In addition, while we focused on a rate-based model, the deployment of NRL on physical hardware like Intel Loihi [8] requires its extension to spiking neural networks (SNNs). Furthermore, the simplicity of our RPE calculation limits its robustness in more complex tasks requiring long-term planning. Future development should incorporate more sophisticated temporal difference learning mechanisms [54, 56], such as a learned value function within an actor-critic architecture [28], to provide a richer temporally sensitive estimate of rewards. Finally, while backpropagation may offer faster convergence in unconstrained settings, recent studies [7, 13], including ours, indicate that this gap can be narrowed for specific networks and tasks.

Our findings ultimately highlight the potential for unifying optimization methods and neurobiological principles. By drawing inspiration from both domains, we have developed a learning rule that not only offers an alternative to backpropagation but is also algorithmically suited for low-energy, event-driven neuromorphic hardware. In the same way, the constraints of biological realism can guide the development of more efficient and robust artificial learning algorithms. This synergistic approach provides a crucial new path for creating low-energy, fast, and adaptive AI systems [68, 36].

Acknowledgments

This publication is part of the DBI2 project (024.005.022, Gravitation), which is financed by the Dutch Ministry of Education (OCW) via the Dutch Research Council (NWO).

References

- [1] Andrew G Barto, Richard S Sutton, and Charles W Anderson. Neuronlike adaptive elements that can solve difficult learning control problems. *IEEE Transactions on Systems, Man, and Cybernetics*, (5):834–846, 1983.
- [2] Atılım Güneş Baydin, Barak A Pearlmutter, Don Syme, Frank Wood, and Philip Torr. Gradients without backpropagation. *arXiv preprint arXiv:2202.08587*, 2022.

- [3] Greg Brockman, Vicki Cheung, Ludwig Pettersson, Jonas Schneider, John Schulman, Jie Tang, and Wojciech Zaremba. OpenAI Gym. *arXiv preprint arXiv:1606.01540*, 10, 2016.
- [4] Jeroen Burms, Ken Caluwaerts, and Joni Dambre. Reward-modulated hebbian plasticity as leverage for partially embodied control in compliant robotics. *Frontiers in Neurobotics*, 9:9, 2015.
- [5] Gert Cauwenberghs. A fast stochastic error-descent algorithm for supervised learning and optimization. *Advances in Neural Information Processing Systems*, 5, 1992.
- [6] Aochuan Chen, Yimeng Zhang, Jinghan Jia, James Diffenderfer, Jiancheng Liu, Konstantinos Parasyris, Yihua Zhang, Zheng Zhang, Bhavya Kailkhura, and Sijia Liu. Deepzero: Scaling up zeroth-order optimization for deep model training. *arXiv preprint arXiv:2310.02025*, 2023.
- [7] Sander Dalm, Marcel van Gerven, and Nasir Ahmad. Effective learning with node perturbation in deep neural networks. *arXiv preprint arXiv:2310.00965*, 2023.
- [8] Mike Davies, Narayan Srinivasa, Tsung-Han Lin, Gautham Chinya, Yongqiang Cao, Sri Harsha Choday, Georgios Dimou, Prasad Joshi, Nabil Imam, Shweta Jain, et al. Loihi: A neuromorphic manycore processor with on-chip learning. *IEEE Micro*, 38(1):82–99, 2018.
- [9] Amir Dembo and Thomas Kailath. Model-free distributed learning. *IEEE Transactions on Neural Networks*, 1(1):58–70, 1990.
- [10] Steve K Esser, Rathinakumar Appuswamy, Paul Merolla, John V Arthur, and Dharmendra S Modha. Backpropagation for energy-efficient neuromorphic computing. *Advances in Neural Information Processing Systems*, 28, 2015.
- [11] A Aldo Faisal, Luc PJ Selen, and Daniel M Wolpert. Noise in the nervous system. *Nature Reviews Neuroscience*, 9(4):292–303, 2008.
- [12] Jesús García Fernández, Nasir Ahmad, and Marcel Van Gerven. Ornstein-Uhlenbeck adaptation as a mechanism for learning in brains and machines. *Entropy*, 26:1125, 2024.
- [13] Jesús García Fernández, Sander Keemink, and Marcel van Gerven. Gradient-free training of recurrent neural networks using random perturbations. *Frontiers in Neuroscience*, 18:1439155, 2024.
- [14] Silvia Ferrari, Bhavesh Mehta, Gianluca Di Muro, Antonius MJ VanDongen, and Craig Henriquez. Biologically realizable reward-modulated hebbian training for spiking neural networks. In *2008 IEEE International Joint Conference on Neural Networks (IEEE World Congress on Computational Intelligence)*, pages 1780–1786. IEEE, 2008.
- [15] Ila R Fiete and H Sebastian Seung. Gradient learning in spiking neural networks by dynamic perturbation of conductances. *Physical Review Letters*, 97(4):048104, 2006.
- [16] C.D. Fiorillo, P.N. Tobler, and W. Schultz. Discrete coding of reward probability and uncertainty by dopamine neurons. *Science*, 299(5614):1898–1902, 2003.
- [17] József Fiser, Pietro Berkes, Gergő Orbán, and Máté Lengyel. Statistically optimal perception and learning: from behavior to neural representations. *Trends in Cognitive Sciences*, 14(3):119–130, 2010.
- [18] Barry Flower and Marwan Jabri. Summed weight neuron perturbation: An $O(n)$ improvement over weight perturbation. *Advances in Neural Information Processing Systems*, 5, 1992.
- [19] Louis Fournier, Stéphane Rivaud, Eugene Belilovsky, Michael Eickenberg, and Edouard Oyallon. Can forward gradient match backpropagation? In *International Conference on Machine Learning*, pages 10249–10264. PMLR, 2023.
- [20] Nicolas Frémaux and Wulfram Gerstner. Neuromodulated spike-timing-dependent plasticity, and theory of three-factor learning rules. *Frontiers in Neural Circuits*, 9:85, 2016.

- [21] Apostolos P Georgopoulos, Andrew B Schwartz, and Ronald E Kettner. Neuronal population coding of movement direction. *Science*, 233(4771):1416–1419, 1986.
- [22] Wulfram Gerstner, Marco Lehmann, Vasiliki Liakoni, Dane Corneil, and Johanni Brea. Eligibility traces and plasticity on behavioral time scales: experimental support of neohebbian three-factor learning rules. *Frontiers in Neural Circuits*, 12:53, 2018.
- [23] Naoki Hiratani, Yash Mehta, Timothy Lillicrap, and Peter E Latham. On the stability and scalability of node perturbation learning. *Advances in Neural Information Processing Systems*, 35:31929–31941, 2022.
- [24] Bernd Illing, Wulfram Gerstner, and Johanni Brea. Biologically plausible deep learning—but how far can we go with shallow networks? *Neural Networks*, 118:90–101, 2019.
- [25] Eugene M Izhikevich. Solving the distal reward problem through linkage of stdp and dopamine signaling. *Cerebral Cortex*, 17(10):2443–2452, 2007.
- [26] Leslie Pack Kaelbling, Michael L Littman, and Andrew W Moore. Reinforcement learning: A survey. *Journal of Artificial Intelligence Research*, 4:237–285, 1996.
- [27] Yuji Kawai and Minoru Asada. Spatiotemporal motor learning with reward-modulated hebbian plasticity in modular reservoir computing. *Neurocomputing*, 558:126740, 2023.
- [28] Vijay Konda and John Tsitsiklis. Actor-critic algorithms. *Advances in Neural Information Processing Systems*, 12, 1999.
- [29] Dhiresha Kudithipudi, Catherine Schuman, Craig M Vineyard, Tej Pandit, Cory Merkel, Rajkumar Kubendran, James B Aimone, Garrick Orchard, Christian Mayr, Ryad Benosman, et al. Neuromorphic computing at scale. *Nature*, 637(8047):801–812, 2025.
- [30] Łukasz Kuśmierz, Takuya Isomura, and Taro Toyozumi. Learning with three factors: modulating hebbian plasticity with errors. *Current Opinion in Neurobiology*, 46:170–177, 2017.
- [31] Pawel Ladosz, Lilian Weng, Minwoo Kim, and Hyondong Oh. Exploration in deep reinforcement learning: A survey. *Information Fusion*, 85:1–22, 2022.
- [32] Dong-Hyun Lee, Shuang Zhang, Asja Fischer, and Yoshua Bengio. Difference target propagation. *European Conference on Machine Learning and Principles and Practice of Knowledge Discovery in Databases (ECML-PKDD)*, pages 498–515, 2015.
- [33] Robert Legenstein, Steven M Chase, Andrew B Schwartz, and Wolfgang Maass. A reward-modulated hebbian learning rule can explain experimentally observed network reorganization in a brain control task. *Journal of Neuroscience*, 30(25):8400–8410, 2010.
- [34] Sijia Liu, Pin-Yu Chen, Bhavya Kailkhura, Gaoyuan Zhang, Alfred O Hero III, and Pramod K Varshney. A primer on zeroth-order optimization in signal processing and machine learning: Principals, recent advances, and applications. *IEEE Signal Processing Magazine*, 37(5):43–54, 2020.
- [35] Wolfgang Maass. Noise as a resource for computation and learning in networks of spiking neurons. *Proceedings of the IEEE*, 102(5):860–880, 2014.
- [36] Adam H Marblestone, Greg Wayne, and Konrad P Kording. Toward an integration of deep learning and neuroscience. *Frontiers in Computational Neuroscience*, 10:215943, 2016.
- [37] Mark D McDonnell and Lawrence M Ward. The benefits of noise in neural systems: bridging theory and experiment. *Nature Reviews Neuroscience*, 12(7):415–425, 2011.
- [38] Thomas Miconi. Biologically plausible learning in recurrent neural networks reproduces neural dynamics observed during cognitive tasks. *Elife*, 6:e20899, 2017.
- [39] Manuel Molano-Mazon, Joao Barbosa, Jordi Pastor-Ciurana, Marta Fradera, Ru-Yuan Zhang, Jeremy Forest, Jorge del Pozo Lerida, Li Ji-An, Christopher J Cueva, Jaime de la Rocha, et al. NeuroGym: An open resource for developing and sharing neuroscience tasks. *PsyArXiv*, 2022.

- [40] P Read Montague, Peter Dayan, and Terrence J Sejnowski. A framework for mesencephalic dopamine systems based on predictive hebbian learning. *Journal of Neuroscience*, 16(5):1936–1947, 1996.
- [41] Emre O Neftci, Charles Augustine, Somnath Paul, and Georgios Detorakis. Event-driven random back-propagation: Enabling neuromorphic deep learning machines. *Frontiers in Neuroscience*, 11:324, 2017.
- [42] John P O’Doherty, Jeffrey Cockburn, and Wolfgang M Pauli. Learning, reward, and decision making. *Annual Review of Psychology*, 68(1):73–100, 2017.
- [43] Adam Paszke, Sam Gross, Francisco Massa, Adam Lerer, James Bradbury, Gregory Chanan, Trevor Killeen, Zeming Lin, Natalia Gimelshein, Luca Antiga, et al. Pytorch: An imperative style, high-performance deep learning library. *Advances in Neural Information Processing Systems*, 32, 2019.
- [44] David Patterson, Joseph Gonzalez, Quoc Le, Chen Liang, Lluís-Miquel Munguia, Daniel Rothchild, David So, Maud Texier, and Jeff Dean. Carbon emissions and large neural network training. *arXiv preprint arXiv:2104.10350*, 2021.
- [45] Kaushik Roy, Akhilesh Jaiswal, and Priyadarshini Panda. Towards spike-based machine intelligence with neuromorphic computing. *Nature*, 575(7784):607–617, 2019.
- [46] David E Rumelhart, Geoffrey E Hinton, and Ronald J Williams. Learning representations by back-propagating errors. *Nature*, 323(6088):533–536, 1986.
- [47] Samuel Schmidgall, Rojin Ziaei, Jascha Achterberg, Louis Kirsch, S Hajiseyedrazi, and Jason Eshraghian. Brain-inspired learning in artificial neural networks: a review. *APL Machine Learning*, 2(2), 2024.
- [48] Wolfram Schultz. Dopamine reward prediction error coding. *Dialogues in Clinical Neuroscience*, 18(1):23–32, 2016.
- [49] Wolfram Schultz, Peter Dayan, and P Read Montague. A neural substrate of prediction and reward. *Science*, 275(5306):1593–1599, 1997.
- [50] Catherine D Schuman, Shruti R Kulkarni, Maryam Parsa, J Parker Mitchell, Bill Kay, et al. Opportunities for neuromorphic computing algorithms and applications. *Nature Computational Science*, 2(1):10–19, 2022.
- [51] H Sebastian Seung. Learning in spiking neural networks by reinforcement of stochastic synaptic transmission. *Neuron*, 40(6):1063–1073, 2003.
- [52] Raghubir Singh and Sukhpal Singh Gill. Edge AI: A survey. *Internet of Things and Cyber-Physical Systems*, 3:71–92, 2023.
- [53] Richard B Stein, E Roderich Gossen, and Kelvin E Jones. Neuronal variability: noise or part of the signal? *Nature Reviews Neuroscience*, 6(5):389–397, 2005.
- [54] Richard S Sutton. Learning to predict by the methods of temporal differences. *Machine Learning*, 3:9–44, 1988.
- [55] Richard S Sutton. Generalization in reinforcement learning: Successful examples using sparse coarse coding. *Advances in Neural Information Processing Systems*, 8, 1995.
- [56] Richard S Sutton. *Reinforcement Learning: An Introduction*. The MIT Press, 2018.
- [57] Richard S Sutton, David McAllester, Satinder Singh, and Yishay Mansour. Policy gradient methods for reinforcement learning with function approximation. *Advances in Neural Information Processing Systems*, 12, 1999.
- [58] Amirhossein Tavanaei, Masoud Ghodrati, Saeed Reza Kheradpisheh, Timothée Masquelier, and Anthony Maida. Deep learning in spiking neural networks. *Neural Networks*, 111:47–63, 2019.

- [59] John Von Neumann. First draft of a report on the edvac. *IEEE Annals of the History of Computing*, 15(4):27–75, 1993.
- [60] Xubin Wang and Weijia Jia. Optimizing edge ai: a comprehensive survey on data, model, and system strategies. *arXiv preprint arXiv:2501.03265*, 2025.
- [61] Paul J Werbos. Backpropagation through time: what it does and how to do it. *Proceedings of the IEEE*, 78(10):1550–1560, 2002.
- [62] Justin Werfel, Xiaohui Xie, and H Seung. Learning curves for stochastic gradient descent in linear feedforward networks. *Advances in Neural Information Processing Systems*, 16, 2003.
- [63] James CR Whittington and Rafal Bogacz. An approximation of the error backpropagation algorithm in a predictive coding network with local hebbian synaptic plasticity. *Neural Computation*, 29(5):1229–1262, 2017.
- [64] James CR Whittington and Rafal Bogacz. Theories of error back-propagation in the brain. *Trends in Cognitive Sciences*, 23(3):235–250, 2019.
- [65] Ronald J Williams. Simple statistical gradient-following algorithms for connectionist reinforcement learning. *Machine Learning*, 8:229–256, 1992.
- [66] Kashu Yamazaki, Viet-Khoa Vo-Ho, Darshan Bulsara, and Ngan Le. Spiking neural networks and their applications: A review. *Brain Sciences*, 12(7):863, 2022.
- [67] Zexiang Yi, Jing Lian, Qidong Liu, Hegui Zhu, Dong Liang, and Jizhao Liu. Learning rules in spiking neural networks: A survey. *Neurocomputing*, 531:163–179, 2023.
- [68] Anthony Zador, Sean Escola, Blake Richards, Bence Ölveczky, Yoshua Bengio, Kwabena Boahen, Matthew Botvinick, Dmitri Chklovskii, Anne Churchland, Claudia Clopath, et al. Catalyzing next-generation artificial intelligence through neuroai. *Nature Communications*, 14(1):1597, 2023.
- [69] Paul Züge, Christian Klos, and Raoul-Martin Memmesheimer. Weight versus node perturbation learning in temporally extended tasks: Weight perturbation often performs similarly or better. *Physical Review X*, 13(2):021006, 2023.

A Gradient approximation using directional derivatives

Consider a function $g(\theta)$, where $\theta = (W_1, \dots, W_L)$ are its parameters. The gradient of this function is defined as follows:

Definition A.1. *The gradient ∇g is a vector indicating the direction of the steepest ascent of the function g , with components as partial derivatives of $g(\theta)$:*

$$\nabla g = \left[\frac{\partial g}{\partial \theta} \right]^\top = \left[\frac{\partial g}{\partial W_1}, \dots, \frac{\partial g}{\partial W_L} \right]^\top. \quad (22)$$

While ∇g captures the rate of change of g in the steepest direction, a directional derivative gives the rate of change in a specified direction. For a unit vector $v = \epsilon / \|\epsilon\|$, normalized via the Euclidean norm, we define the directional derivative as:

Definition A.2. *The directional derivative of $g(\theta)$ along a unit vector $v = (v_1, \dots, v_n)$ is defined by the limit*

$$\nabla_v g(\theta) = \lim_{h \rightarrow 0} \frac{g(\theta + hv) - g(\theta)}{h}, \quad (23)$$

where h is a small step size.

For a sufficiently small h we numerically measure the directional derivative as

$$\nabla_\epsilon g(\theta) = \frac{g(\theta + h\epsilon) - g(\theta)}{h\|\epsilon\|}. \quad (24)$$

This directional derivative can also be measured as a projection of ∇g in the direction v , following the relation:

$$\nabla_v g(\theta) = v \cdot \nabla g(\theta). \quad (25)$$

We can now formally demonstrate how gradients can be approximated using directional derivatives.

Theorem A.3. *Let $\epsilon \sim \mathcal{N}(0, \sigma^2 I_n)$ (probability distribution $p(\epsilon)$) where n is the number of dimensions in θ . Exact gradients can be written in terms of directional derivatives using expectations*

$$\nabla g(\theta) = n \mathbb{E}_{p(\epsilon)} [v^\top \nabla_v g(\theta)]. \quad (26)$$

Proof.

$$\begin{aligned} \nabla g(\theta) &= n \mathbb{E}_{p(\epsilon)} [v^\top \nabla_v g(\theta)] \\ &= n \mathbb{E}_{p(\epsilon)} [vv^\top \nabla g(\theta)] \\ &= n \mathbb{E}_{p(\epsilon)} [vv^\top] \nabla g(\theta) \\ &= n \mathbb{E}_{p(\epsilon)} \left[\frac{\epsilon}{\|\epsilon\|} \frac{\epsilon^\top}{\|\epsilon\|} \right] \nabla g(\theta) \\ &= n \frac{1}{n} I_n \nabla g(\theta) = \nabla g(\theta) \end{aligned}$$

as we assume $p(\epsilon) = \mathcal{N}(0, \sigma^2 I_n)$, which gives $\mathbb{E}[vv^\top] = \mathbb{E} \left[\frac{\epsilon}{\|\epsilon\|} \frac{\epsilon^\top}{\|\epsilon\|} \right] = \frac{1}{n} I_n$. \square

Now, consider gradient descent in the direction of the gradient $\nabla g(\theta)$ as

$$\theta_{t+1} = \theta_t + \alpha \nabla g(\theta_t). \quad (27)$$

This update can be reformulated using directional derivatives.

Theorem A.4. *Let $\eta = \frac{\alpha n}{hK}$ and $\epsilon^{(i)} \sim \mathcal{N}(0, \sigma^2 I_n)$. Gradient descent is equivalent to the update rule*

$$\theta_{t+1} = \theta_t + \alpha \sum_{i=1}^K \left[\frac{\epsilon^{(i)}}{h\|\epsilon^{(i)}\|^2} \left[g(\theta + h\epsilon^{(i)}) - g(\theta) \right]^\top \right] \quad (28)$$

in the limit when $h \rightarrow 0$ and $K \rightarrow \infty$.

Proof.

$$\begin{aligned}
\nabla g(\theta) &= n\mathbb{E}_{p(\epsilon)} [v\nabla_v g(\theta)^\top] \\
&= \lim_{h \rightarrow 0} n\mathbb{E}_{p(\epsilon)} \left[v \left[\frac{g(\theta + h\epsilon) - g(\theta)}{h\|\epsilon\|} \right]^\top \right] \\
&= \lim_{h \rightarrow 0} n\mathbb{E}_{p(\epsilon)} \left[\frac{\epsilon}{\|\epsilon\|} \left[\frac{g(\theta + h\epsilon) - g(\theta)}{h\|\epsilon\|} \right]^\top \right] \\
&= \lim_{h \rightarrow 0} n\mathbb{E}_{p(\epsilon)} \left[\frac{\epsilon}{h\|\epsilon\|^2} [g(\theta + h\epsilon) - g(\theta)]^\top \right].
\end{aligned}$$

Now, substituting the expectation with a sampling under some empirical distribution:

$$\nabla g(\theta) = \lim_{h \rightarrow 0} \lim_{K \rightarrow \text{inf}} \frac{n}{hK} \sum_{i=1}^K \left[\frac{\epsilon^{(i)}}{\|\epsilon^{(i)}\|^2} [g(\theta + \epsilon^{(i)}) - g(\theta)]^\top \right].$$

Finally, defining gradient descent on parameters θ as $\theta_{t+1} = \theta_t + \alpha \nabla g(\theta)$:

$$\begin{aligned}
\theta_{t+1} &= \theta_t + \alpha \nabla g(\theta) \\
&= \alpha \lim_{h \rightarrow 0} \lim_{K \rightarrow \text{inf}} \frac{n}{hK} \sum_{i=1}^K \left[\frac{\epsilon^{(i)}}{\|\epsilon^{(i)}\|^2} [g(\theta + \epsilon^{(i)}) - g(\theta)]^\top \right] \\
&= \lim_{h \rightarrow 0} \lim_{K \rightarrow \text{inf}} \frac{\alpha n}{hK} \sum_{i=1}^K \left[\frac{\epsilon^{(i)}}{\|\epsilon^{(i)}\|^2} [g(\theta + \epsilon^{(i)}) - g(\theta)]^\top \right].
\end{aligned}$$

□

In practice, small perturbations, controlled by h , and limited numbers of noise samples are sufficient to approximate the gradient. For $K = 1$, analogous to single-sample updates in stochastic gradient descent:

$$\theta_{t+1} = \theta_t + \eta \frac{\epsilon}{\|\epsilon\|^2} \rho \tag{29}$$

with $\rho = [g(\theta + h\epsilon) - g(\theta)]^\top$.

B Model hyperparameters and training details

All hyperparameters were carefully tuned per method and problem to ensure fair comparisons across methods. The number of episodes was chosen to illustrate the convergence of our method relative to baseline methods, with 8000, 20000, and 1000 episodes used for the Acrobot, Cartpole, and Reaching problems, respectively. In all our experiments, we set the smoothing factor for reward estimation to $\lambda = 0.66$, striking a balance between recent values (for quick adaptability) and a longer history (for robustness against rapid reward fluctuations). Each neural network consisted of an input, hidden, and output layer. Input units corresponded to environment observation elements, and output units to possible actions. Specifically, Acrobot, Cartpole, and Reaching used 6, 4, and 32 input units and 3, 2, and 2 output units, respectively, with hidden layer sizes of 64, 64, and 128. Table 2 summarizes the learning rate η and noise standard deviation σ for each method and problem. Higher values of these parameters could lead to unstable training, while lower values may result in slower learning.

Table 2: Learning rate η and noise standard deviation σ for the different learning algorithms across problems. Dashes indicate that the parameter is not used.

| | | BP | Ours | RMHL |
|-----------------|----------|-----------|-------------|-------------|
| Acrobot | η | 5e-3 | 5e-2 | 5e-2 |
| | σ | - | 1e-3 | 1e-3 |
| Cartpole | η | 5e-3 | 5e-2 | 1e-2 |
| | σ | - | 1e-3 | 1e-1 |
| Reaching | η | 1e-2 | 1e-2 | 1e-1 |
| | σ | - | 1e-3 | 1e-1 |